CrossMark

ORIGINAL ARTICLE

Modeling of soil loss and its impact factors in the Guijiang Karst River Basin in Southern China

Ping Chen[1] · Yanqing Lian[2]

Abstract The Guijiang Karst River Basin (GKRB) is a typical karst river basin in southern China and one of the major tributaries to the Xijiang River in the Pearl River Basin. A portion of the main stem in the upper reach of GKRB is called the Li River known for its most scenic karst landforms in the world. Soil erosion has resulted in rocky desertification in karst areas of the basin. Excessive sediment load in rivers would affect tourism navigation in the Li River and the aquatic systems in the basin. This study employed the Revised Universal Soil Loss Equation Version 2(RUSLE2) model to estimate soil loss and to evaluate the impact factors for the spatial and temporal variation of soil erosion in the basin. The GKRB RUSLE2 model was calibrated with sediment yields from nine gaging stations with the Nash–Sutcliffe efficiency coefficient (NSE) as high as 0.69. This study showed that soil erosion occurred on 54.9 % of the land areas that are primarily forest and cropland and in low hills with elevations ranging from 30 to 600 m. It also showed that the soil erosion rate is higher in areas where the degree of rocky desertification is more severe, indicating area with high soil erosion intensity often has high risk of rocky desertification. Impacted by monsoons, soil erosion in the study basin showed clear seasonal variation. The second quarter of the year had highest erosion rate, mostly due to the intensive late spring and early summer rainstorms. This study has shown that the RUSLE2 model can be used for karst river basin with reasonable accuracy. Findings from this study may help in identifying locations for flow and sediment control structures to reduce the risk of soil erosion and subsequently rocky desertification.

Keywords Guijiang River Basin · Soil erosion · Karst · Rocky desertification

Introduction

Soil erosion is the wearing of top soil by water flow or wind. It is a naturally occurring process on all land. Soil erosion may be a slow process that continues unnoticed. Unfortunately, human activities such as farming and timbering have accelerated soil erosion in many places on the earth. When soil is eroded drastically at an extent exceeding the capacity of soil system recovery, irreversible destruction on ecological systems would take place. To protect farmlands from accelerated soil erosion, the U.S. Department of Agriculture (USDA) established soil loss tolerance values or T values, against which to evaluate "acceptable" rates of soil erosion in the 1950s (Schertz 1983). In 1965, the USDA published its first version of the Universal Soil Loss Equation (USLE) to estimate the soil loss. USLE is based on extensive erosion data from studies throughout the USA and provides a quick approach to estimating long-term average annual soil loss (A) and it is now widely used around the world to estimate soil erosion by raindrop impact and surface runoff. Other more physically based soil erosion models were developed to accommodate particular and local conditions at scales

✉ Yanqing Lian
ylian@illinois.edu

Ping Chen
cp_chenping@126.com

[1] School of Geographical Sciences, Southwest University, No. 1, Tiansheng Road, Beibei District, Chongqing 400715, People's Republic of China

[2] University of Illinois at Urbana-Champaign, Champaign, IL, USA

Springer

ranging from individual field and small catchment to watershed or administrative unit. WEPP (Water Erosion Prediction Project, Flanagan et al. 2007), EUROSEM (European Soil Erosion Model, Morgan et al. 1998) are more for field or catchment scale. ANSWERS (Areal Non-point Source Watershed Environment Response Simulation; Russell et al. 1998), LISEM (Limburg Soil Erosion Model; DeRoo and Offermans 1995) and PESERA (Pan-European Soil Erosion Risk Assessment; Licciardello et al. 2009) are more suitable for drainage basin scale.

Karst systems are ecologically fragile due to their unique geological and geomorphological feature and geochemical components (Cai 1989). Carbonate rock is highly soluble and not able to produce much soil (Jiang et al. 2014). Cai (1989) estimated that the annual soil formation rate was about 11 ton per square kilometer, which is far less than other types of soil in non-carbonate rock areas in China. A research by Su (2002) indicates that it would take 4–8.5 thousand years to form 1 cm thick soil layer in karst areas in Guizhou, China, which implies it would be extremely difficult to recover the soil layer once lost in karst areas (Jiang et al. 2014). The double or triple structure of pores, fractures, and karst conduits in karst systems complicate hydrological processes. Water retaining capacities in soil layers are low due to the high permeability of fractures and other karst features (Yuan and Cai 1988), which results in the absence of soil moisture for vegetation growth. Areas with less dense surface streams tend to have more soil erosion (Jiang et al. 2011). Karst soil environments consequently are more vulnerable than other landscapes. Human interventions on karst terrain systems trigger chain reactions on soil loss and land degradation, which is eventually characterized by the area of exposed rocks and rocky desertification.

Soil erosion models are mostly developed with focus on soil erosion processes in non-karst agricultural lands. Applications of soil erosion modeling for karst watersheds and river basins are limited. However, studies by Xu et al. (2007), Xiong (2009), Ni et al. (2010), and Wang (2011) showed reasonably good performances of USLE and RUSLE in karst areas. Xu et al. (2007), Geissen et al. (2007), Kheir et al. (2008), and Yang et al. (2014) used RUSLE model and field investigation methods to assess soil erosion risk in karst areas by including karst desertification index and rock infiltration index that accounts for the lithology, lineament density, karstification and drainage density. Febles-Gonzalez et al. (2011) and Feng et al. (2014) have used the Morgan–Morgan–Finney (MMF) model and the revised MMF model successfully in karst areas as well.

The main objectives of this study were to develop a soil erosion model for the GKRB to validate the application of RUSLE2 model for the karst river basin and to understand the spatial and temporal characteristics of soil erosion in the GKRB. The calibrated RUSLE2 model will be used to evaluate the impact factors such as rainfall intensity, topography, and land use/cover to soil erosion rates in the GKRB.

Study area

The Guijiang River Basin is located in the northeast part of the Guangxi Zhuang Autonomous Region (GZAR) between the longitudes of $110°05' \sim 110°29'$ east and latitudes of $23°28' \sim 25°55'$ north (Fig. 1). The total basin area is about 19,288 km^2 and the main stem of the Guijiang River extends for 426 km from north to south. The Guijiang River originates from the Maoer (Cat) mountain at 2141 m above the mean sea level (m-a.s.l.). To its north is the Yuecheng Ling Mountain which separates the Yangtze River and the Pearl River systems. About 40.9 % of the basin is karst area, which is primarily located in the lower upper and middle reach of the basin. The rest non-karst areas are mainly in the lower reach of the basin (Fig. 1). A portion in the middle reach of the Guijiang River is called the Li River, which is famous for the well-developed karst features including karst forests and several levels of karst caves that form the most beautiful karst scenes in the world (Zhang et al. 2012). Guijiang River ends at the confluence with the Xijiang River as part of the Pearl River Delta drainage system.

Located in the subtropical region, the climate condition of GKRB is clearly affected by monsoons. The annual average precipitation in the basin is around $1900 \sim 2700$ mm. About 78 % of the total annual precipitation is from March to August. Precipitation from April to June can be as high as 50 % of the total.

On the regional scale, as part of the contributing watersheds to the Pearl River basin, the quantity and quality of flow and sediment from the Guijiang River have direct and profound impacts to the social and economic development, water security, and ecosystems in the Pearl River Delta. The Li River, the karst landscapes and karst caves nearby are the unique tourism resources for tourists in China and around the world and are the major revenue both for Guilin and Yangshuo cities. Low water levels and excessive sediment load in the river particularly in some dry years have already affected the tourism. GKRB has been established as an Ecological Function Zone for water conservation and biodiversity in 2012 (Guangxi Development and Reform Committee 2012), which would bring financial opportunities for rocky desertification control and restoration of a healthy ecological environment within the basin.
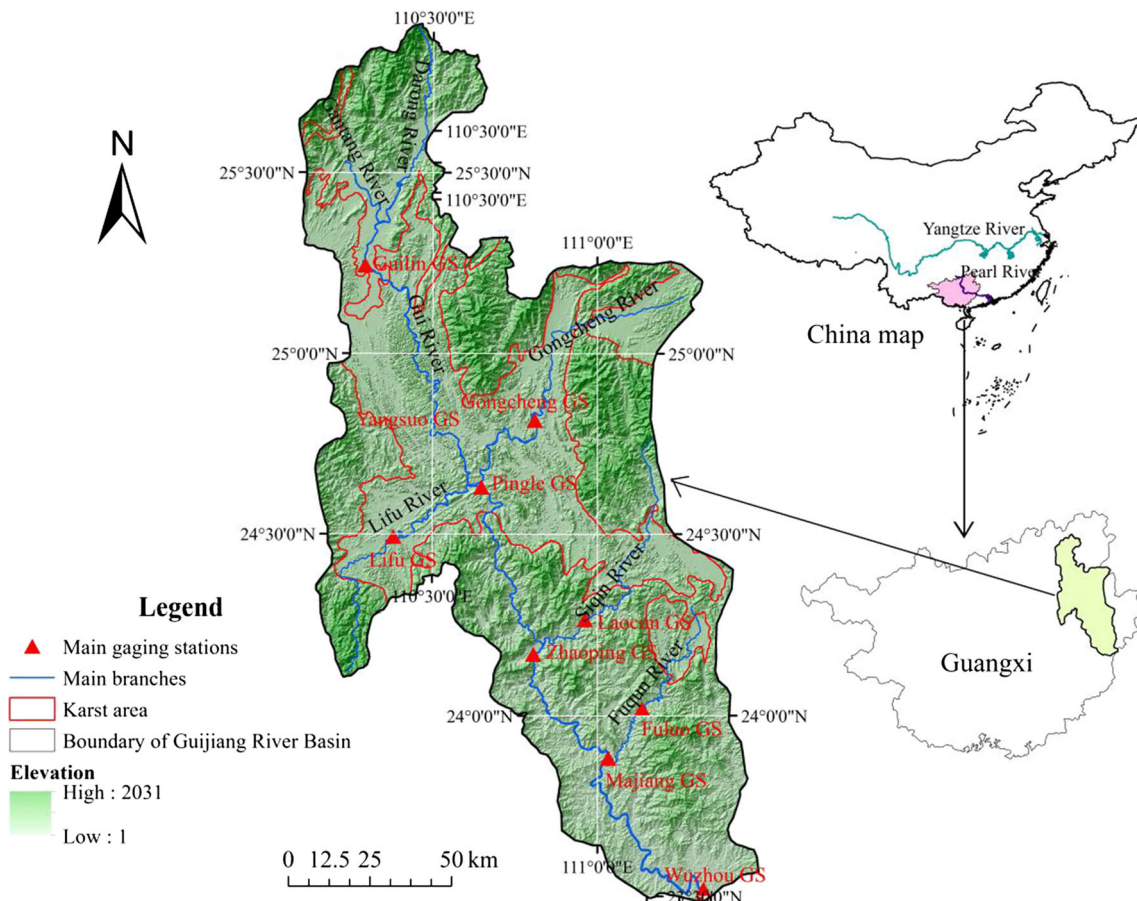
Fig. 1 Topography and major rivers in the Guijiang Karst River Basin. The *upper right map* displays the location of GZAR in China. The *lower right map* shows the study area in GZAR

Methodology and data

This study used the Revised Universal Soil Loss Equation Version 2 (RUSLE2) to estimate the intensity of soil erosion together with GIS technology to analyze and classify topographic features for distributed modeling.

The revised universal soil loss equation version 2—RUSLE2

The revised universal soil loss equation version 2 (RUSLE2) is an improved version of the soil erosion estimation model—USLE (Universal Soil Loss Equation) developed by the U.S. Department of Agriculture (USDA) Soil Conservation Service (now the USDA Natural Resources Conservation Service, Wischmeier and Smith 1978) based on soil erosion data collected beginning from the 1940s in the USA. The model has been used for decades for purposes of conservation planning both in the USA and around the world and has been used to help implement the USA multi-billion dollar conservation programs. The USLE

was entirely an empirically based equation and was limited in its application to conditions where experimental data were available for deriving factor values. The revised universal soil loss equation (RUSLE) was released in the early 1990s (Renard et al. 1997). RUSLE or refereed as RESULE1 is land use independent and can be applied to any land use having exposed mineral soil and Hortonian overland flow. RUSLE2 was released in mid-2003 and it is also land use independent. It uses the USLE basic formulation for the unit plot but expanded from estimating annual average soil loss rate to daily time steps. RUSLE2 uses a set of mathematical equations to compute erosion, thus the erosion estimates are site-specific which allows erosion control practices to be tailored to each specific site. This mathematic form of RUSLE2 is on a daily basis and is expressed as (Renard et al. 1997):

$$A = R \times K \times L \times S \times C \times P \tag{1}$$

in which A is average annual soil loss ($t/(ha \times yr)$), R is average soil erosivity factor ($MJ \times mm/(ha \times h \times yr)$), K is the soil erodibility factor ($t \times ha \times h/(ha \times MJ \times mm)$), L is soil length factor (dimensionless), S is

slope steepness factor (dimensionless), C is cover-management factor (dimensionless) and P is supporting practice factor (dimensionless). Major factors affecting soil erosion include climate (rainfall), soil, topography and land use, indicated by R-factor, K-factor, LS-factor, C-factor, and P-factor, respectively.

R-factor is the rainfall erosivity factor reflecting the effect from both rainfall amount and rainfall intensity. The average annual erosivity is the product of total energy and the maximum 30 min intensity of individual storms. However, the raw data for this computation are very difficult to obtain. In practice a series of methods to compute the average annual erosivity through daily, monthly and yearly precipitation were developed as an estimation. In this study, a model based on daily rainfall proposed by Guo et al. (2001) was employed to calculate the monthly and yearly average rainfall erosivity. A sine function was used to approximate the seasonal fluctuations of rainfall in subtropical monsoon climate zone, where major rainstorms occur in the summer months. Thus, the R-factor can be computed as following:

$$R_Y = 0.0043 \left[1 + 48.13 \sin\left(\frac{\pi}{12(j-1)}\right) \right] \sum_{k=1}^{N} P_k^{1.09} \quad (2)$$

$$\text{with } P_k > P_0$$

where R_Y is average annual erosivity, j stands for the month, P_0 is of the threshold for a storm to be erosive. The threshold was set as 12.7 mm (Ning and Shi 2003) in this study, P_k is daily rainfall (mm), N is the number of days when daily rainfall is greater than the threshold P_0 in a month, and k represents the kth storm with a rainfall greater than the threshold P_0 in a month. Values for N are less than 31 and k varies from 1 to N.

K-factor is soil erodibility that reflects the soil susceptibility to detachment and transportation during erosion. Values for K-factor typically range from about 0.013 to 0.059 SI units (Foster et al. 1981), with high-sand and high-clay content soils having the lower values and high-silt content soils having the higher values. K-factor was computed using the Erosion-Productivity Impact Calculator (EPIC) model proposed by Williams et al. (1984):

the 1:1,000,000 scale soil thematic map of China for all types of soils.

LS-factor is the slope length (L) and slope steepness (S) and is computed with the equation developed by McCool et al. (1989):

$$\begin{aligned} L &= (\lambda / 22.1)^\alpha \\ \alpha &= \beta (\beta + 1) \\ \beta &= (\sin \theta / 0.0896)/[3.0 \sin^{0.8} \theta + 0.56] \end{aligned} \quad (4)$$

where L is slope length factor, slope length λ is the horizontal projection (m) and USLE uses 22.13 m for the unit plot, α is slope length exponent, β represents ratio of rill to inter-rill erosion, and θ is slope angle. When θ varies from 0 to 60°, β ranges from 0 to 2.99 and α from 0 to 0.750.

Slope steepness factor S was computed by the equation developed by McCool et al. (1987) and Liu et al. (1994). S can be calculated by the following equations:

$$\begin{cases} S = 10.8 \times \sin \theta + 0.03 & \theta < 5° \\ S = 16.8 \times \sin \theta - 0.50 & 5° \le \theta \le 14° \\ S = 21.9 \times \sin \theta - 0.96 & \theta > 14° \end{cases} \quad (5)$$

C-factor is a dimensionless value to represent the effect of cropping, vegetation and management practices on erosion rates in a particular site (Liu et al. 2010). The C-factor is perhaps the most important USLE/RUSLE factor because it represents conditions that can most easily be managed to reduce erosion. Values for C-factor can vary from near zero for very well-protected soil to 1.5 for finely tilled surface that produces much runoff and leaves the soil highly susceptible to rill erosion (McCool et al. 1995). Field data are often required to calculate C-factor directly. In practice C-factor is commonly determined from land use/cover. RUSLE2 uses a subfactor method to compute values for the cover-management factor C in a distributed fashion, thus to account for the impact of land use to soil erosion for specific sites. Unfortunately, this study was for a very large basin and was also a reconnaissance application of RUSLE2 model for a karst river basin; data for the rigorous use of RUSLE2 were limited. In this study, values for the C-factor were treat as a constant. The initial C-

$$\begin{aligned} K_{EPIC} = &\left\{ 0.2 + 0.3 \exp\left[0.0256 \text{SAN}\left(1 - \frac{\text{SIL}}{100}\right) \right] \right\} \left(\frac{\text{SIL}}{\text{CLA} + \text{SIL}} \right)^{0.3} \\ &\left(1.0 - \frac{0.25C}{C + \exp(3.17 - 2095C)}\right) \left(1.0 - \frac{0.7SN1}{SN1 + \exp(-5.51 + 22.9SN1)}\right) / 7.59 \end{aligned} \quad (3)$$

where SAN, SIL, CLA, and C are the percentages of content of sand, silt, clay and organic carbon, respectively; $SN1 = 1 - SAN/100$. Parameters in Eq. (3) are included in

factor values for this study were obtained from published studies in similar type of conditions in southwestern China (Zeng 2008; Ni et al. 2010). The final estimation of C-

factor value for each land use type was obtained from calibration.

P-factor accounts for support practices that will affect erosion by affecting runoff. Support practices often include contouring (ridging), barriers (vegetative strips, silt fences), flow interceptors (diversions), sediment basins, and subsurface drainage (Foster et al. 2003). Terraces are often built in the GRKB on hill slopes for rice crops and to prevent runoff and soil loss.

RUSLE2 uses equations that are functions of ground cover, soil biomass, surface roughness, and soil consolidation. The effectiveness of contouring is computed as a function of runoff and slope steepness. Critical slope length, the location where contouring fails, is computed as a function of the shear stress applied to the soil. RUSLE2 uses runoff in process-based equations to compute deposition caused by concave slopes, barriers, and low-grade channels (Foster et al. 2003). Unfortunately, the detailed information that is required by RUSLE2 was not available for GRKB for the current study. Values for *P*-factors were obtained from calibration.

Evaluation of model performance

Modeling accuracy for soil loss is affected by parameter uncertainties in the RUSLE2 model. The model performance for calibration and validation was evaluated by the Nash–Sutcliffe Efficiency Coefficient (NSE). NSE is expressed as the following:

$$NSE = 1 - \frac{\sum_{i=1}^{n} (L_0^i - L_m^i)^2}{\sum_{i=1}^{n} (L_0^i - \overline{L_o^i})^2} \qquad (6)$$

where: L_0^i is transformed soil loss rate by observed sediment discharge of the gaging station i, $\overline{L_0^i}$ is the mean of L_0^i, L_m^i is modeled soil loss rate. NSE ranges from $-\infty$ to 1.0 (1 inclusive), with NSE of 1 being the optimal value. Values from 0 to 1.0 are generally viewed as acceptable levels of performance, whereas values less than 0 indicate that the mean observed value is a better predictor than simulated value, which indicates unacceptable performance (Moriasi et al. 2007).

Data for the study

The climate data (precipitation for this study) for the 25 meteorological stations in GZAR from 1951 to 2010 were obtained from the China Meteorological Administration. The digital elevation model (DEM) data were derived from the free data of Shuttle Radar Topography Mission (SRTM) (at 90 m resolution). The land use/cover data were

from the 1:100,000 scale thematic map in 2000. The 1:1,750,000 scale geologic map for the GZAR was from the Institute of Geology, Chinese Academy of Geological Sciences. The 1:250,000 scale fundamental geographical information data for the GZAR were from the National Geomatics Center of China. The 1:1,000,000 scale Chinese soil thematic map was from the Institute of Soil Science, Chinese Academy of Sciences. The Landsat 5 TM satellite imageries acquired on Oct 1st, 2001 were downloaded from the USGS website (http://www.usgs.gov/pubprod/). The average cloud coverage for these images was below 3 %. Sediment load data used for model calibration were collected from published papers and reports (Yang et al. 2003; Wang 2013).

RUSLE2 model for the Guijiang River Basin

The RUSLE2 modeling of the Guijiang River Basin in this study was based entirely on GIS. Figure 2 shows the major procedures for data preparation, model calibration and analyses of impact factors to soil erosion rates for this study. Six raster maps for *R*-, *K*-, *L*-, *S*-, *C*-, and *P*- factors were all generated in ArcGIS.

The R-factor was computed based on the daily rainfall data from 1951–2010. The multi-year averaged monthly soil erosivity was computed from the Eq. (2). The multi-year averaged annual soil erosivity was then the sum of monthly erosivities. These annual average erosivities at 25 meteorological stations were used to generate a continuous surface of *R*-factor grid layer for GKRB using ordinary kriging interpolation function under the ArcToolbox. For the *K*-factor, raster files for SAN, SIL, CLA and C (please note this C is not the *C*-factor) were derived from the soil thematic map by converting vector to raster. A grid layer for the *K*-factor described in Eq. (3) was then generated using the raster algebra function in the ArcToolbox. For the *L*-factor, a raster for λ was created by processing DEM using the Hydrology tools in ArcToolbox. Raster maps for β, a, and L listed in Eq. (4) were then subsequently derived using the raster algebra function in ArcToolbox. A grid layer for the *S*-factor was derived using the similar procedure to the *L*-factor but using Eq. (5). Raster maps for the *C*- and *P*-factors were derived from the calibrated values for each land use. With grid layers for all six parameters created, a soil erosion rate map for the RUSLE2 model can be created by multiplying these six factors. The zonal statistics tool in ArcGIS was used to calculate the average soil erosion rate for the drainage area of each soil loss monitoring station.

The multi-year annual averaged observed sediment discharge data from the nine gaging stations in the study area were collected. The observed sediment discharge data were then converted into soil loss rate (Table 2) using a
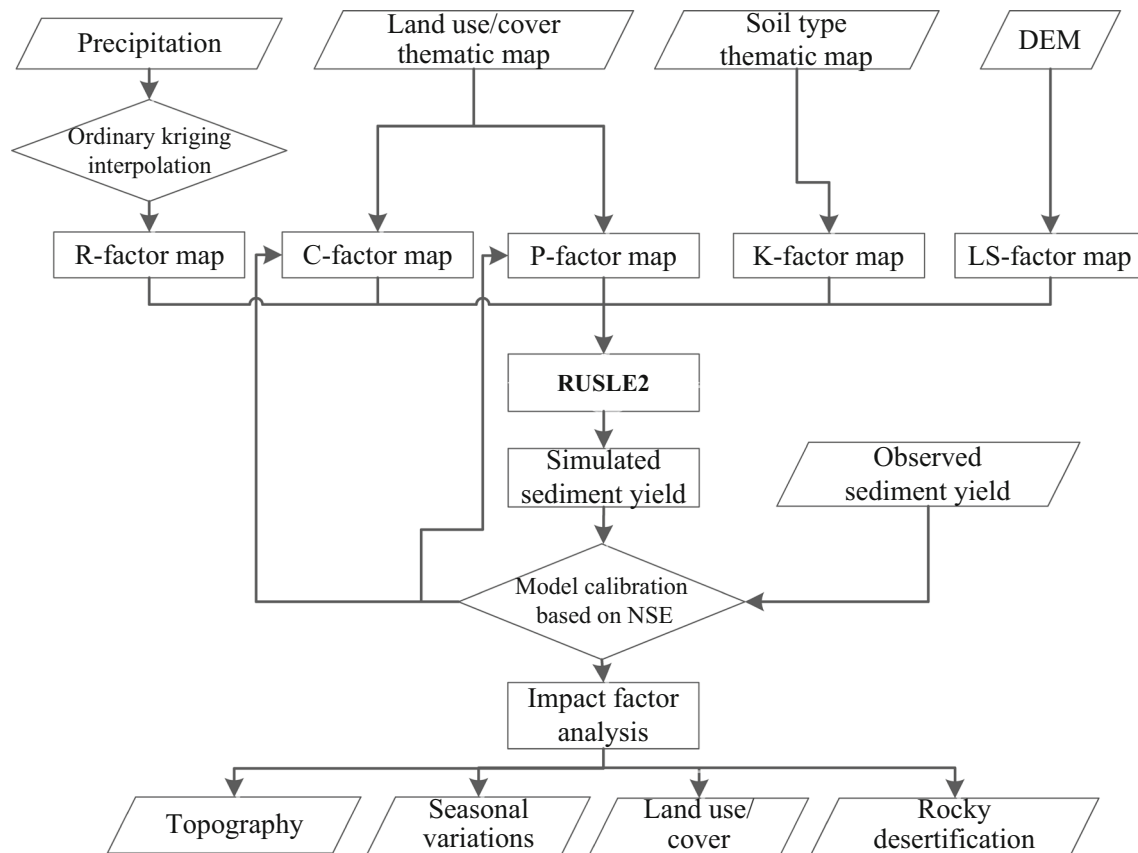
Fig. 2 A flowchart of procedures for the development of RUSLE2 model in ArcGIS

sediment delivery ratio of 0.9 (Wang 2013). Modeling accuracy was evaluated using the NSE.

Out of the six parameters in the model, K-, L-, and S-factors are more related to the physical characteristics of the study basin and were treated as fixed and were computed using GIS. As stated earlier, although the intention was to use the sophisticated RUSLE2 model for GRKB, data were limited to performing convincing computation for C- and P-factor; therefore, parameter values for C- and P-factors had to be calibrated. Initial values for the C- and P-factors were adopted from references (Fernandez et al. 2003; Ismail and Ravichandran 2008; Zeng 2008; Ni et al. 2010) for the same or similar type of land uses and support practices. For example, initial values for the C-factor were based on the work by Ni et al. (2010) and Zeng (2008), which unfortunately resulted in a NSE as low as −0.41. No reliable data to narrow the range of P-factor values during calibration, this study, however, tried to keep the relative importance of various support practices in preventing soil erosion. For example, the rice crop land use should have lower soil loss than dry land crop and lower P-factor value. Presumably land use practices in the karst and non-karst areas are different as landforms can be drastically different,

different sets of C- and P-factor values were used for the karst and non-karst areas in the calibration (Table 1). Calibration of C- and P-factor values focused more on the dominant land uses as listed in Table 1.

With tedious manual calibration, the best NSE achieved in the calibration was as high as 0.69 (Table 2). It can be seen in Table 2 that the absolute relative errors for six sub-basins were around or below 15 %. Unfortunately, the relative errors for the Fuluo and Lipu sub-basins were as high as 25.3 and 24.5 %, respectively, which was due to their complicated karst landforms and also because of the selection of parameter values in favor of better modeling accuracy for the entire basin. Nonetheless, areas for Fuluo and Lipu sub-basins are less than 5 % of the total basin area; their high relative errors did not have major impact to the overall modeling error for the GKRB. With over-estimation in some sub-basins but under-estimation in other sub-basins, the overall relative error was as low as 0.64 %. The coefficient of determination between modeled and observed soil erosion rates was about 0.71 (Fig. 3). This calibrated model was then applied to analyze the impact of various factors to soil erosion rates in the GKRB with confidence.

Table 1 Calibrated C-factor and P-factor values for different land use/cover

Land use/cover classification		Karst area			Non-karst area		
Level I	Level II	Percent Area (%)	C-factor	P-factor	Percent Area (%)	C-factor	P-factor
Cropland	Paddy field	11.83	0.005	0.5	4.92	0.02	0.45
	Rained paddy	0.03	0.04	0.7	0.01	0.045	0.7
	Dry land	2.05	0.045	0.6	0.26	0.06	0.7
	Vegetable field	0.01	0.045	0.6	0.05	0.06	0.7
Garden	Orchard	0.21	0.038	0.7	0.09	0.06	0.7
	Tea garden	0	0.04	0.7	0.01	0.05	0.7
	Rubber estate	0	0.04	0.7	0.01	0.04	0.7
Forest	Forest land	8.64	0.005	0.7	48.2	0.01	0.8
	Shrub wood	4.35	0.006	0.8	1.05	0.02	0.8
	Open forest	0.58	0.008	0.8	1.33	0.025	0.85
	Immature forest	0.52	0.025	1	2.31	0.059	1
	Slash	0.06	0.028	1	0.13	0.035	1
	Nursery garden	0.09	0.02	0.9	0.01	0.02	0.9
Grassland	Grassland	0.68	0.003	1	0.41	0.003	1
Unused land	Wild grassland	1.24	0.001	1	4.29	0.0012	1
	Bared land	0.01	0.02	1	0	0	0
	Bared rock	4.92	0	0	0.33	0	0
Build-up land	Build-up land	0.33	0	0	0.42	0	0
Water body	Water body	0.13	0	0	0.49	0	0

Detailed sub-types for build-up land and water body are not included in the table; the values of C- and P-factor for these sub-types were set as 0

Table 2 Modeling accuracy of RUSLE2 for the Guijiang Karst River Basin

Gaging station	Area of Sub-basin (km^2)	Percent area of Sub-basin			Observed soil loss rate [t/(km^2·yr)]	Modeled soil loss rate [t/(km^2·yr)]	Absolute error [t/(km^2·yr)]	Relative error (%)	NSE
		Karst (%)	Non-karst (%)	Total					
Guilin	2523	2.74	10.35	13.09	142.8	164.68	21.88	15.32	0.69
Lipu	892	1.97	2.65	4.62	133.8	166.55	32.75	24.47	
Gongcheng	2588	6.91	6.51	13.42	230.0	201.28	−28.72	−12.49	
Pingle	5791	22.30	7.72	30.02	93.9	104.96	11.06	11.78	
Majiang	1391	0.00	7.21	7.21	156.2	134.70	−21.52	−13.77	
Zhaoping	1366	1.06	6.02	7.08	268.7	230.55	−38.12	−14.19	
Laocun	1634	4.03	4.44	8.47	174.4	148.11	−26.29	−15.07	
Fuluo	624	1.84	1.39	3.23	144.4	180.95	36.55	25.31	
Wuzhou	2480	0.00	12.86	12.86	175.8	154.31	−21.52	−12.24	
Entire Basin	19288	40.85	59.15	100	156.7	157.70	1.00	0.64	

As a common practice for model development, the calibrated parameters, particularly the *C*- and *P*-factors, would need to be validated with a new set of data or data for different time period(s). Unfortunately this study was not able to obtain the time series data or even the data of different time periods for soil loss in the river basin for RUSLE2 model validation.

Results and discussion

Estimation of soil loss in the Guijiang River Basin

Ministry of Water Resources of China has published a national standard for classification and ranking of soil erosion in 1997 and a revised edition in 2008.
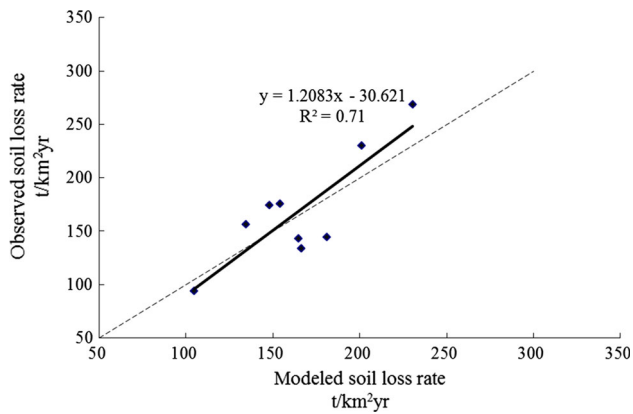
Fig. 3 The Correlation of modeled soil loss rate and observed soil loss rate from the nine gaging stations in the Guijiang Karst River Basin. The *dashed line* is a 45° reference and the *solid line* is the *fitted line* from data

Unfortunately, those standards are unable to accurately reflect the severity of soil erosion in karst areas (Cao et al. 2008). Cao et al. (2008) then developed a new set of criteria to classify the intensity of soil erosion for karst areas in southwest China. Columns 1 and 2 in Table 3 are the classification of soil loss intensity and their corresponding soil loss defined by Cao et al. (2008). Table 3 shows soil erosion occurred in about 54.9 % of the basin area with an average soil erosion rate of 157.7 t/(km^2 × yr) and an average annual soil loss up to 3.0 × 10^6 ton. About 70.8 % of this 54.9 % soil erosion areas or 38.9 % of the total basin area had micro to medium degree erosion and the soil loss from these areas was about 15.2 % of the total soil loss in the basin. About 16.0 % of the basin area had strong to severe soil erosion and contributed about 84.8 % of the total soil loss in the GKRB. A comparison of percent area experienced soil erosion in karst and non-karst areas shows that soil loss in karst area was much less than non-karst areas, largely due to the less farming in karst land. Soil loss from non-karst areas with soil loss intensity higher than

medium intensity was almost 4–6 times more than karst areas, largely due to high percentage of exposed carbonate rocks and lack of soil in the karst terrains that is typical in the southwest karst area of China (Jiang et al. 2014). Figure 4 shows the spatial distribution of different soil erosion classes listed in Table 3. It can be seen areas with soil loss more than 200 t/(km^2 × yr) were mainly distributed in the high-elevation non-karst areas, such as the north of the basin, the south and northwest mountain areas of the Gongcheng River. The spatial distribution of soil loss from this study was consistent with the high sediment load data collected at the Gongcheng gaging station (Wang 2013).

Impact factors of soil erosion in the Guijiang River Basin

Soil erosion is often affected by natural factors such as topography and climate conditions and human activities for social and economic development and land use/cover practices. Soil erosion in karst areas would result in rocky desertification; on the other hand areas of rocky desertification are more susceptible to soil erosion.

Seasonal variation

The GKRB is located in a typical subtropical monsoon climate zone characterized by rainfall concentrated from spring to summer seasons. Small rainstorms do not necessarily result in soil loss. The threshold for rainfall with a capability of erosivity was set as 12.7 mm for the study area. The monthly rainfall and monthly *R*-factor in Fig. 5 are for rainfalls greater than the threshold. Figure 5 shows that the curves of the monthly *R*-factor and rainfall have similar shape, indicating the monthly *R*-factor varies with rainfall in the basin. Listed in Table 4 are the soil losses for the four quarters in a calendar year. The seasonal soil loss was computed using the monthly averaged *R*-factor values and the annual average for other factors.

Table 3 Statistics of simulated soil loss in the Guijiang Karst River Basin

Category of soil loss intensity	Soil loss intensity [t/(km^2·yr)]	Percentage of land area with soil loss			Total soil loss (t/yr)		Percent of soil loss (%)	
		Karst area	Non-karst area	Total area	Karst area	Non-karst area	Karst area	Non-karst area
Non	0	19.62	25.50	45.12	0	0	0.00	0.00
Micro	0 ~ 30	11.67	4.97	16.64	15,758	10,139	0.52	0.33
Slight	30 ~ 100	4.73	6.66	11.39	53,191	83,443	1.76	2.75
Medium	100 ~ 200	2.32	8.53	10.85	62,572	236,750	2.06	7.81
Strong	200 ~ 500	1.63	8.05	9.68	96,301	482,569	3.18	15.93
Highly strong	500 ~ 1000	0.52	3.06	3.58	70,565	407,249	2.33	13.44
Severe	>1000	0.36	2.38	2.74	212,289	1,299,421	7.01	42.88
Total		40.85	59.15	100	510,677	2,519,571	16.85	83.15

Fig. 4 Spatial distribution of categories of soil erosion intensity in the Guijiang Karst River Basin
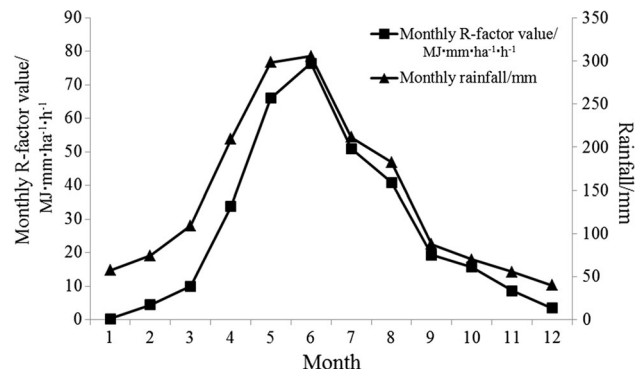

Fig. 5 Comparison of multi-year monthly average rainfall and monthly *R*-factor in the Guijiang Karst River Basin

August (Wang 2013). The estimated sediment load from March to August from this study was about 82.6 % of the annual soil loss. In addition, this study showed the change of *R*-factor value was only between 83.2 and 82.6 % when the threshold rainfalls altered from 9.2 mm, 12.7 mm to 15 mm, indicating that *R*-factor was not very sensitive to soil erosion.

Topography

Jiang et al. (2014) reviewed that topography in karst areas has great impact to soil erosion. Vegetation cover on steep slopes in karst areas is often low due to lack of soil and soil moisture. The higher gravity force from overland flow in steep slope areas increases the erodibility and carrying capacity of sediments. The average land surface slope in the GKRB is around 13.6°. GKRB is characterized by mature karst landforms such as Fengcong and Fenglin (http://www.goodearthgraphics.com/virtcave/karst/karst.html). It is typical that the land surface in the karst basin undulates and the land surface slopes have a wide range of variations. This landform variation can be better characterized by terrain undulation than by land surface slopes. Thus, the terrain undulation instead of land surface slopes was used in this study. Terrain undulation was defined as the difference of elevations between a target point and its surrounding areas and was processed by neighborhood operation using ERDAS IMAGINE 9.2, a remote sensing application for geospatial raster data processing and analysis. Computation of terrain undulation is performed by selecting a target pixel in the DEM image as a center so to create an 11 × 11-pixel matrix (kernel) as an analyzing window, the maximum difference of elevations between the central pixel and neighboring pixels within the kernel is then the terrain undulation. The same procedure is applied to all pixels to eventually generate a raster map of terrain undulations. Landforms were then classified into plain

It can be seen in Table 4 that rainfall from January to March is about 14.1 % of the annual rainfall but the corresponding *R*-factor is as low as 4.5 %, which implies some rainfall events in the period were unable to erode soil. Whereas the percentage of *R*-factor for the months of April to September was 87.1 % for the rainfall percentage of 76.1 % for the period, indicating more soil loss in the GKRB was due to the large amount of rainfall and more importantly high rainfall intensity in the second and third quarters of the year. The total soil loss in the second quarter was as high as 53.4 % and soil loss in the summer season (July–September) was about one-third of the annual average soil loss. The GKRB hardly experiences snow in winter seasons, the soil erosion loss for the 6 months from October to January was as low as 8.5 %, which was mostly due to rainfall in late fall and early spring.

An analysis by Wang (2013) on the sediment discharge data from gaging stations of Guilin, Gongcheng, Lipu and Pingle in the GKRB showed that 90 ∼ 97.6 % of sediment discharge occurred in the flood season from March to

Table 4 Statistics of quarterly average soil loss in the Guijiang Karst River Basin

Month	Percent to annual average rainfall (%)	Percent to annual R-factor (%)	Intensity of soil erosion [t/(km²·yr)]	Total soil loss (t/yr)	Percent to annual soil loss (%)
Jan ~ Mar	14.14	4.46	7.03	143,634	4.74
Apr ~ Jun	47.81	53.42	84.24	1,621,183	53.50
Jul ~ Sept	28.32	33.71	53.16	1,009,073	33.30
Oct ~ Dec	9.73	8.40	13.25	256,359	8.46

area, hilly area, highland area, mountainous land area, and high mountainous land area as shown in Fig. 6.

Listed in Table 5 are soil losses from different landforms in the GKRB. This river basin can be characterized as hilly and high land with about 40.8 % hilly areas and 42.8 % of highland areas. Areas with terrain undulation more than 600 m are less than 1 % and plain areas are about 5.6 %. The average intensity of soil erosion increased as the terrain undulation increased. About 55.8 % of the soil loss was from highland areas. As high as 98.1 % of the soil loss was from land with undulation from 30 to 600 m.

Land use/cover

There were eight land use/cover classes in the GKRB, i.e. forest land, cropland, garden land, grassland, built-up land, transportation land, water body and unused land (Fig. 7). Forest land was as high as 67.3 % in the basin. 19.2 % was cropland for rice and corn. Grassland was about 1.1 % and the garden land was merely 0.3 %. About 1.4 % of the land composed of built-up land, transportation land and water bodies were assumed no soil erosion (Table 6). The average soil erosion intensity for the forestland was as high as 218.5 t/(km² × yr). Soil loss from forest and cropland accounted for 86.4 % of total land area and contributed about 98.9 % of the total soil loss. Soil loss from garden land and grass land and unused land was merely 1.1 %.

Forest lands are located in the hilly, highland, and mountainous land areas which proportions for 33, 51.5, and 13.9 %, respectively. Hilly areas are mostly covered by orchards and economic forests. Pinewoods and bamboo forests are major species in the mountainous lands within the basin (Department of Agriculture of GZAR 2008). Results from this study showed that properly managing these two types of land use/cover within the basin would be crucial for soil loss control. The cropland located in plain, hilly, and highland area was about 21.3, 66, and 12.5 %, respectively. The cropland for growing corn is typically acidic, lack of cohesiveness to the bedrock, and with thin soil layer and low soil moisture content, and also lack of water infrastructures. All these features would make the
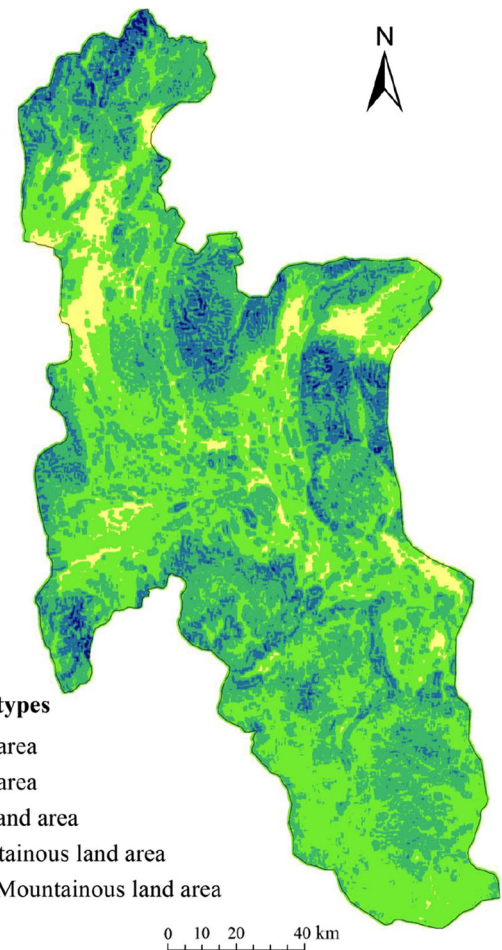

Fig. 6 Spatial distribution of different types of landforms in the Guijiang Karst River Basin

land more vulnerable to soil loss and consequently rocky desertification if in the karst area (Planning and Compilation Group and Zhang 2008).

Rocky desertification

Rocky desertification is used to characterize the processes that transform a karst area covered by vegetation and soil into a rocky landscape almost devoid of soil and vegetation (Yuan 1997). Rocky desertification is the ultimate

Table 5 Statistics of Soil loss for different terrain undulation in the Guijiang Karst River Basin

Category of Terrain undulation (m)	Landform type	Area (km²)	Areal ratio (%)	Average intensity of soil erosion [t/(km²·yr)]	Total soil loss (t/yr)	Ratio of annual soil loss (%)
0~30	Plain area	1103	5.58	1.34	1,365	0.05
30~200	Hilly area	8073	40.80	71.62	553,428	18.26
200~400	Highland area	8458	42.75	203.25	1,692,132	55.84
400~600	Mountainous land area	2023	10.23	361.15	727,566	24.01
>600	High mountainous land area	128	0.65	436.05	55,757	1.84

Table 6 Statistics of soil loss for different types of land use/cover in the Guijiang Karst River Basin

Types of land use/cover	Area (km²)	Areal ratio (%)	Average soil erosion rate [t/(km²·yr)]			Total soil loss (t/yr)	Ratio of annual soil loss (%)
			Karst area	Non-karst area	Average		
Forest	12918	67.25	57.62	261.70	218.49	2,822,986	93.16
Cropland	3684	19.18	27.75	98.67	47.14	173,717	5.73
Unused land	2071	10.8	1.89	20.89	10.00	20,724	0.68
Grass land	211	1.10	21.39	42.06	29.14	6,136	0.20
Garden land	63	0.33	96.41	128.72	106.68	6,686	0.22
Others*	2610	1.36	0	0	0	0	0

* Others include the built-up land, transportation land, and water bodies, which are assumed no soil erosion

consequence of soil erosion. However, the degree of rocky desertification would affect soil erosion largely due to land slopes and lack of vegetation cover. Figure 8 shows the distribution of the 40.9 % of the karst and 59.1 % of the non-karst areas in the river basin. Karst areas are mostly located in the plain and hilly areas in the north central and northwest of the GKRB. Overall the estimated soil loss from karst areas and non-karst areas was about 16.9 and 83.1 %, respectively. Comparatively, rocky desertification in the GKRB was not as bad as some other regions in southwest China (Jiang et al. 2014). Areas with none, mild, moderate, and severe rocky desertification in the karst areas of the basin were about 58.9, 39.5, 1.6 and 0 %, respectively.

Overall 97.0 % of the total soil loss in karst area occurred in the none and mild karst rocky desertification areas in the basin, out of which 26 and 71 % were from the none and mild rocky desertification areas, respectively. Table 7 shows that the soil erosion intensity increased as the rocky desertification became more severe. Luckily area with moderate rocky desertification was merely 1.6 % and the total soil loss was about 3 % of the total soil loss in karst area. No area in the basin had severe rocky desertification.

Summary and conclusion

A RUSLE2 model was developed for the GKRB to estimate soil erosion rates and was used to evaluate the major factors affecting soil erosion in the basin. This study showed the
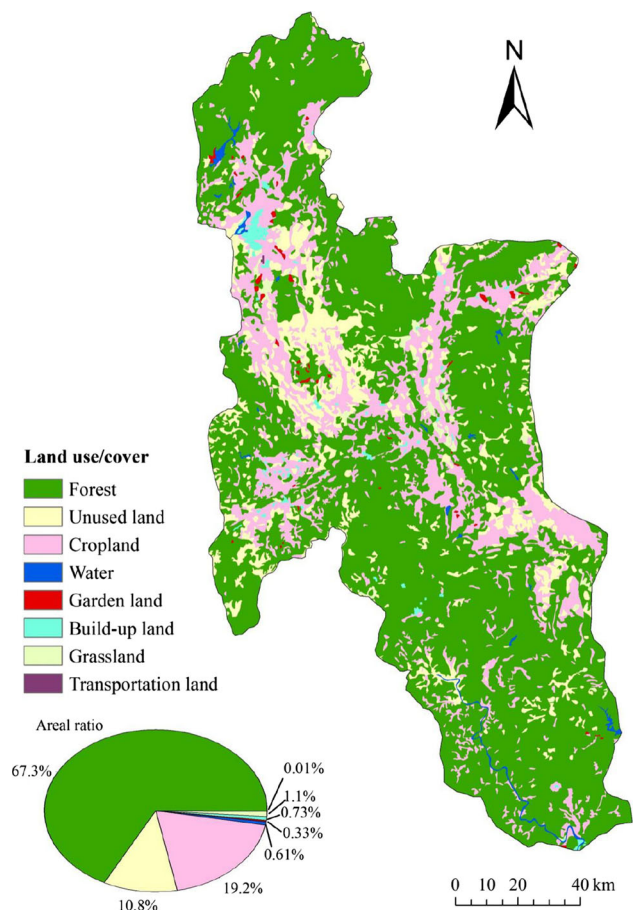

Fig. 7 Spatial distribution and areal percentages of different types of land use/cover in the Guijiang Karst River Basin

Table 7 Statistics of soil loss for karst areas of various degree of rocky desertification in the Guijiang Karst River Basin

Severity of Rocky Desertification	Average land surface slope (°)	Bare rock ratio (%)	Area (km²)	Areal ratio (%)	Average intensity of soil erosion [t/(km²·yr)]	Total soil loss (t/yr)	Ratio of annual soil loss (%)
None	<= 12	<= 30	4631	58.92	133,398	28.81	26.11
Mild	12 ~ 25	30 ~ 50	3103	39.49	362,592	116.85	70.97
Moderate	25 ~ 35	50 ~ 70	125	1.59	14,893	119.08	2.92
Severe	>35	>70	0	0		0	0
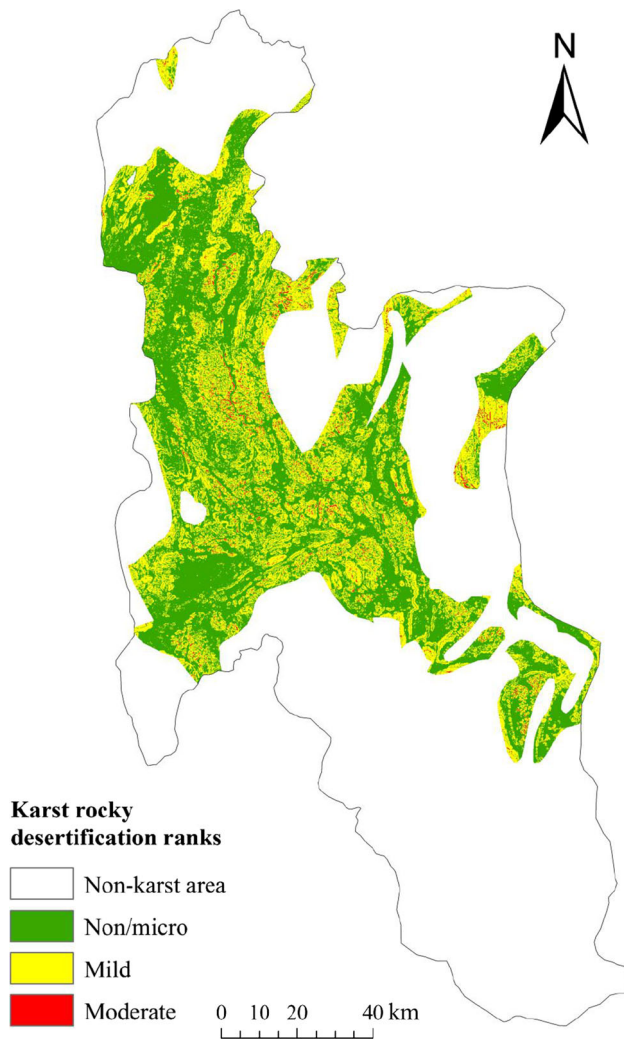
Fig. 8 Spatial distribution of karst rocky desertification in the Guijiang Karst River Basin

RUSLE2 can be used for karst river basin with some confidence. The relative error between modeled and observed soil loss rates for 7 out of 9 sub-basins was around or below 15 %. With over-estimation in some sub-basins but under-estimation in others the overall relative error for the entire GKRB was as low as 0.64 %. The best NSE achieved in the calibration was as high as 0.69, and the coefficient of determination between them was about 0.72.

Overall, this river basin experiences medium erosion, with average soil erosion rate of about 157.7 t/(km² × yr) and an average annual soil loss up to 3.0×10^6 ton. On the average, soil erosion from non-karst (59.1 %) and kart areas (40.9 %) contributes about 83.1 and 16.9 % of the total soil loss, respectively; 84.0 % of the land surface areas in the basin experience none to medium soil erosion. Areas with strong, highly strong and severe soil erosion intensities were mainly distributed in the high-elevation non-karst areas, such as the north of the basin, the south and northwest mountain areas of the Gongcheng River, which yield 84.8 % of the total soil loss.

This study showed that rainfall and rainfall intensity has dominant impact to the seasonal variation of soil erosion. Small and low intensity rains from October of the previous year to March of the following year only contributed about 13.2 % of the total soil loss; 86.8 % of the soil loss was from April to September when major and intensive rainfall occurred.

This river basin has about 40.8 % hilly areas and 42.8 % highland areas. The average intensity of soil erosion increases as terrain undulation increases. About 55.8 % of the soil loss is from highland areas. As high as 98.1 % of the soil loss is from land with undulation from 30 to 600 m. Forest land and cropland were two dominant classes of the land use/cover for about 86.4 % of the total basin and contributed about 98.9 % of the total soil loss. This finding suggests that proper management of these two land use/-cover would be crucial for soil loss control.

Rocky desertification is the ultimate consequence of soil erosion. However, the degree of rocky desertification would affect soil erosion largely due to land slopes and lack of vegetation cover. The study showed that the soil erosion intensity increased as the rocky desertification became more severe. Average total soil loss from areas without rocky desertification was about 26.1 and 71.0 % from areas with mild karst rocky desertification. Soil loss from areas with moderate rocky desertification was around 3.0 %, largely due to high percentage of exposed carbonate rocks and lack of soil in the karst terrains that is typical in the southwest karst area of China.

As a reconnaissance investigation of the RULSE2 model for the karst river basin, this study intended to use RUSLE2

for its full advantage for the GKRB. Unfortunately, some of the parameters and sub-data sets for the *C*- and *P*-factors were not available for this study. RUSLE2 model is a physically and land independent model but also a heavily data driven model. More studies are necessary for better data modeling accuracy. Nonetheless, the finding on the spatial distribution of soil erosion scales can identify areas of high rocky desertification risk and information on the seasonal variation of soil erosion and sediment load in streams can help to build flow and sediment control structures to reduce the risk of soil erosion and subsequently rocky desertification. Estimated soil erosion can be used to estimate the organic carbon in the soil that is often considered as a major factor for carbon sequestration of karst systems in southwest China.

References

Cai ZX (1989) Soil erosion in karst area of Guangxi. Mt Res 7(4):255–260 **(in Chinese)**

Cao JH, Jiang ZC, Yang DS, Pei JG, Yang H, Luo WQ (2008) Grading of soil erosion intensity in Southwest karst area of China. Sci Soil Water Conserv 6(6):1–7 **(in Chinese)**

DeRoo APJ, Offermans RJE (1995) LISEM: a physically-based hydrological and soil erosion model for basin-scale water and sediment management. Model Manag Sustain Basin-scale Water Resour Syst 231:399–407

Febles-Gonzalez JM, Vega-Carreno MB, Tolo-Becerra A, Lastra-Bravo X (2011) Assessment of soil erosion in karst regions of Havana, Cuba. Land Degrad Dev 23(5):465–474

Feng T, Chen HS, Wang KL, Zhang W, Qi XK (2014) Modeling soil erosion using a spatially distributed model in a karst catchment of northwest Guangxi, China. Earth Surf Proc Land 39(15):2121–2130

Fernandez C, Wu JQ, McCool DK, Stockle CO (2003) Estimating water erosion and sediment yield with GIS, RUSLE, and SEDD. J Soil Water Conserv Soc 58(3):128–136

Flanagan DC, Gilley JE, Franti TG (2007) Water Erosion Prediction Project (WEPP): Development history, model capabilities, and future enhancements. Trans ASAE 50(5):1603–1612

Foster GR, Lane LJ, Nowlin JD, Laflen JM, Young RA (1981) Estimating Erosion and Sediment Yield on Field-Sized Areas. Trans ASAE 24:1253–1263

Foster GR, Toy TE, Renard KG (2003) Comparison of the USLE, RUSLE1.06c, and RUSLE2 for application to highly disturbed lands. Proceedings of the 1st Interagency Conference on Research in the Watersheds, Benson, Arizona, October 27–30, 2003, 154–160. Washington, DC: USDA Agricultural Research Service

Geissen V, Kampichler C, Llergo-Juárez JJL-d, Galindo-Acántara A (2007) Superficial and subterranean soil erosion in Tabasco, tropical Mexico: Development of a decision tree modeling approach. Geoderma 139:277–287

Guangxi Development and Reform Committee (2012) Guangxi main functional area planning. http://jhw.liuzhou.gov.cn/hgjj/fzgh/201304/P020130427618394506055.doc **(in Chinese)**

Guo XB, Wang ZQ, Zhang RL (2001) Study on temporal distribution of rainfall erosivity and daily rainfall erosivity model in red soil area of Zhejiang. J Soil Water Conserv 15(3):35–37 **(in Chinese)**

Ismail J, Ravichandran S (2008) RUSLE2 model application for soil erosion assessment using remote sensing and GIS. Water Resour Manage 22:83–102

Jiang ZC, Li XK, Hu BQ (2011) Rocky desertification in karst mountainous areas in Guangxi and its comprehensive treatment. Science Publishing House, Beijing

Jiang ZC, Lian YQ, Qin XQ (2014) Rocky desertification in Southwest China: impacts, causes, and restoration. Earth Sci Rev 132:1–12

Kheir RB, Abdallah C, Khawlie M (2008) Assessing soil erosion in Mediterranean karst landscapes of Lebanon using remote sensing and GIS. Eng Geol 99(3–4):239–254

Licciardello F, Govers G, Cerdan O et al (2009) Evaluation of the PESERA model in two contrasting environments. Earth Surf Proc Land 34(5):629–640

Liu BY, Nearing MA, Risse LM (1994) Slope gradient effects on soil loss for steep slopes. Trans ASAE 37(6):1835–1840

McCool DK, Brown LC, Foster GR (1987) Revised slope steepness factor for the universal soil loss equation. Trans ASAE 30(5):1387–1396

McCool DK, Foster GR, Mutchler CK et al (1989) Revised slope length factor for the universal soil loss equation. Trans ASAE 32(5):1571–1576

McCool DK, Foster GR, Renard KG, Yoder DC, Weesies GA (1995) The revised universal soil loss equation. http://www.tucson.ars.ag.gov/unit/publications/PDFfiles/1132.pdf

Morgan RPC, Quinton JN, Smith RE, Govers G, Poesen JWA, Auerswald K, Chisci G, Torri D, Styczen ME (1998) The european soil erosion model (EUROSEM): a dynamic approach for predicting sediment transport from fields and small catchments. Earth Surf Proc Land 23(6):527–544

Moriasi DN, Arnold JG, Liew MWV, Bingner RL, Harmel RD, Veith TL (2007) Model evaluation guidelines for systematic quantification of accuracy in watershed simulations. Trans ASABE 50(3):885–900

Ni JP, Yuan DX, Xie DT, Wei CF (2010) Estimating soil erosion in small watershed of karst valley area using GIS. J Basic Sci Eng 18(2):217–225 **(in Chinese)**

Ning LD, Shi H (2003) Estimating R-factor in Southwest China with data of daily rainfall amount. Res Soil Water Conser 10(4):183–186 **(in Chinese)**

Planning and Compilation Group, Zhang J (2008) Planning for comprehensive desertification control in Karst area of Guangxi Zhuang Autonomous Region. Pratacultural Sci 25(9):93–102 **(in Chinese)**

Renard K, Foster G, Weesies G (1997) Predicting soil erosion by water: A guide to conservation planning with the Revised Universal Soil Loss Equation (RUSLE) In: Agriculture Handbook No. 703, U.S. Department of Agriculture, Washington DC, pp 15

Russell SK, John LK, Paul BD (1998) BASINS: Better assessment science integrating point and non-point sources. U.S. Environmental Protection Agency, Office of Water. Springer, USA, pp 1–24

Schertz DL (1983) The basis for soil loss tolerances. J Soil Water Conserv 38(1):10–14

Su WC (2002) Controlling model for rocky desertification of karst mountainous region and its preventing strategy in Southwest, China. J Soil Water Conserv 16(2):29–32 **(in Chinese)**

Wang R (2011) Study on soil erosion modelling in karst areas. Beijing University, Beijing (in Chinese)

Wang QC (2013) Sediment development and water and soil conservation analysis for Guijiang River basin area within Guilin City. Guangxi Water Resour Hydropower Eng 3(3):56–59 **(in Chinese)**

Williams RJ, Jones AC, Dyke PT (1984) A modeling approach to determining the relationship between erosion and soil productivity. Trans ASAE 27:129–144

Wischmeier WH, Smith D (1978) Predicting rainfall erosion losses-A guide to conservation planning. In: Agriculture Handbook No. 537, U.S. Department of Agriculture, Washington DC, pp 1–17

Xiong YL (2009) Study on RUSLE of soil erosion prediction. Beijing Normal University, Beijing **(in Chinese)**

Xu YQ, Shao XM, Kong XB, Jian P, Cai YL (2007) Adapting the RUSLE and GIS to model soil erosion risk in a mountains karst watershed, Guizhou Province China. Environ Monit Assess 141(1–3):275–286

Yang HL, Luo HX, Ren GL (2003) Simple analysis of the annual erosion modulus characteristics of the various rivers in Wuzhou City and Hezhou Prefecture. GX Water Resour Hydropower Eng 3:11–14 **(in Chinese)**

Yang QY, Xie YQ, Li WJ, Jiang ZC, Li H, Qin XM (2014) Assessing soil erosion risk in karst area using fuzzy modeling and method of the analytical hierarchy process. Environ Earth Sci 71(1):287–292

Yuan DX (1997) Rock desertification in the subtropical karst of south China. Zeitschrift für Geomorphologie 108:81–90

Yuan DX, Cai GH (1988) Karst Environment Chongqing Publish House, Chongqing

Zeng LY (2008) Study on soil erosion in Karst area based on RUSLE Model—a case study of the Catchment of Hongfenghu Lake in Guizhou Province. Beijing University, Beijing **(in Chinese)**

Zhang HB, He SY, Yu S, Wang YX, Wang LL (2012) Hydrochemical characteristics and influencing factors of the river water in the Guijiang. Carsologica Sinica 31(4):395–401 **(in Chinese)**